Protein Science (1993), *2*, 915-926. Cambridge University Press. Printed in the USA.

Brownian dynamics simulations of molecular recognition in an antibody-antigen system

RICHARD E. KOZACK AND SHANKAR SUBRAMANIAM

National Center for Supercomputing Applications, Department of Physiology and Biophysics, and Beckman Institute for Advanced Science and Technology, University of Illinois at Urbana-Champaign, Urbana, Illinois 61801

(RECEIVED December 22, 1992; REVISED MANUSCRIPT RECEIVED February 17, 1993)

Abstract

The crystal structure for an antibody-antigen system, that of the anti-hen egg lysozyme monoclonal antibody HyHEL-5 complexed to lysozyme, is used as the starting point for computer simulations of diffusional encounters between the two proteins. The investigation consists of two parts: first, the linearized Poisson-Boltzmann equation is solved to determine the long-range electrostatic forces between antibody and antigen, and then, the relative motion as influenced by these forces is modeled within Brownian motion theory. The effects of various point mutations on the calculated reaction rate are considered. It is found that charged residues close to the binding site exert the greatest influence in steering the proteins into a configuration favorable for their binding, while more distant mutations are qualitatively described by the Smoluchowski model for the mutual diffusion of two uniformly charged spheres. The antibody residues involved in forming salt links with the lysozyme, Glu-H35 and Glu-H50, appear to be particularly important in electrostatic steering, as neutralization of both of them yields reaction rates that are two to three orders of magnitude below those of wild-type rates. The relative rates obtained from the simulations can be tested through kinetic measurements on mutant protein complexes. Kinetically efficient partners can also be designed and constructed through directed mutagenesis.

Keywords: antibody-antigen complex; Brownian dynamics simulations; diffusion-controlled reactions; electrostatic steering; molecular recognition; Poisson-Boltzmann equation

Molecular recognition in the immune system is extraordinarily specific. Advances in protein crystallography, hybridoma technology, molecular biology, and simulation methodology enable their synergistic use to obtain detailed insight into the antibody-antigen molecular recognition process (Davies et al., 1990). From stopped-flow spectrophotometric measurements of the rate of association and viscosity dependence of the reaction, it has been shown that the association of the monoclonal antibody 2B5 with cytochrome *c* is diffusion controlled (Raman et al., 1992). Also, a theoretical investigation of a model system by Northrup and Erickson (1992) has demonstrated the ability of computer simulations to reproduce the magnitude of the reaction rate expected for protein-protein encounters. These results suggest the application of Brownian dynamics methods for studying the specificity of antibody binding, and in particular for obtaining relative rates of association for wild-type and mutant complexes.

It is our purpose to model the phenomenon of molecular recognition in the immune system, in which an antibody interacts through long-range electrostatic forces with an antigen as it undergoes diffusional motion and steers into a configuration favorable for binding. Molecular recognition is especially suitable for computational study as it can be based on well-established physical models, and one can also, with presently available algorithms and resources, probe time scales of experimental interest. The results presented here can be directly correlated with kinetic experiments, help provide a deeper understanding of the forces that are responsible for recognition, and have implications for design and engineering of antibodies that have enhanced specificity.

The particular system under investigation consists of the monoclonal antibody HyHEL-5 and hen egg lysozyme. A crystal structure of this complex has been obtained to 2.8 Å resolution (Kinemage 1; Sheriff et al., 1987), and experimental results are available for the relative binding

Reprint requests to: Shankar Subramaniam, Beckman Institute, University of Illinois at Urbana-Champaign, 405 N. Mathews Avenue, Urbana, Illinois 61801.

affinities of similar lysozymes from other avian species to HyHEL-5 (Smith-Gill et al., 1982). Work involving designed mutants of these proteins is also underway (Willson, pers. comm.). Aside from this large amount of empirical information, the HyHEL-5–lysozyme system possesses some physical features that make it desirable for an investigation of molecular recognition. The lysozyme has a net total charge of +7e, and the number of contacts in the complex is minimal, being dominated by three salt bridges in a well-defined geometry. The residues involved in these links are Glu-H35 and Glu-H50, which both lie within a groove of the antibody, and Arg-45 and Arg-68 on the lysozyme. An experiment by Smith-Gill et al. (1982) showed that the binding affinity of HyHEL-5 is several orders of magnitude smaller for bobwhite quail lysozyme as compared to hen egg lysozyme. The quail enzyme has Arg-68 replaced with Lys, another positively charged residue. Also, in two directed mutant proteins, one with Arg-68 replaced by Lys and the other with Arg-45 replacing Lys, the I_{50} of the complex was found to be 10,000-fold and 750-fold, respectively, smaller compared to the recombinant native HEL protein (Lavoie et al., 1989). The change in the length of the positively charged side chains alters the local electric fields near the groove, and it might therefore be anticipated that electrostatics plays an important role in the formation of the complex.

Results

Brownian dynamics simulations

The modeling of molecular recognition consists of two parts: first, the long-range electrostatic forces between antibody and antigen are calculated, and then the relative motion of the two proteins as influenced by these forces is simulated. The techniques used for carrying out the relevant computations have been extensively developed and applied by McCammon and co-workers (Davis et al., 1990) and are collectively referred to as Brownian dynamics. The first part is accomplished through a numerical solution of the linearized Poisson-Boltzmann equation:

$$-\nabla\cdot\epsilon\nabla\phi + \epsilon\kappa^2\phi = \rho, \tag{1}$$

where ϵ is the dielectric constant, κ is the inverse Debye length, and ϕ is the electrostatic potential (Gilson & Honig, 1987; Davis & McCammon, 1989). In the above expression, the charge density ρ is determined for the protein configuration obtained from the crystal structure coordinates. The diffusional motion is propagated in discrete time steps, Δt according to the Langevin equation-based algorithm of Ermak and McCammon (1978):

$$\Delta\mathbf{r} = \frac{D}{kT}\mathbf{F}(t)\Delta t + \mathbf{R}(t), \tag{2}$$

where $\Delta\mathbf{r}$ is the change in relative position, kT is the Boltzmann factor, D is the relative diffusion constant, $\mathbf{F}(t)$ gives the electrostatic force obtained from the solution for ϕ, and $\mathbf{R}(t)$ is a random vector satisfying certain statistical constraints. Equation 2 is used to generate a series of trajectories, beginning with an intermolecular separation distance of b and terminating when either a predetermined reaction condition based on interatomic distances is satisfied or when the distance between molecules is equal to q. The determination of the b and q parameters is discussed below. The probability that a trajectory yields a successful reaction, β, can then be used to compute a reaction rate k given by (Northrup et al., 1984):

$$k = \frac{k_s(b)\beta}{1 - (1-\beta)k_s(b)/k_s(q)}, \tag{3}$$

where $k_s(a)$ is the analytical result for the reaction rate for diffusion to a sphere of radius a in a spherically symmetric potential $U(r)$, which obeys the expression

$$k_s(a) = 4\pi D\left\{\int_a^\infty \frac{\exp[U(r)/kT]}{r^2}\,dr\right\}^{-1}. \tag{4}$$

The goal of the present study is to run simulations for a large number of mutants of the HyHEL-5–lysozyme system. This will help to provide understanding on general aspects of antigen recognition, as well as guiding experimentalists as to which residues are important in electrostatic steering. The coordinates of over 4,000 atoms are provided in the crystal structure of the antibody–antigen complex. Although entire protein–protein systems have been simulated through Brownian dynamics (Northrup et al., 1988; Nambi et al., 1991), and work is underway toward that end to obtain reliable absolute reaction rates for the entire antibody–antigen complex, it is not possible to investigate such a wide variety of mutants with presently available computer resources. We therefore consider a model system that is simple enough to allow for extensive investigation of different mutations, yet still contains the essential aspects of the molecular recognition.

The antibody is represented by one of its Fv fragments (residues H1–116 from the heavy chain and L1–105 of the light chain), with coordinates taken from the crystal structure data (Kinemage 1). This portion, which forms an independent domain composed of a light chain and a heavy chain, encompasses the entire active site of the protein and moreover contains all of the complementarity-determining regions of the antibody, which are responsible for its specificity (Kinemage 2). Although it is the case that the rest of the Fab segment of the molecule given in the crystal structure contains charged residues that can affect the electrostatic steering, these are distant from the binding site, and it will be shown that they contribute to

the physics in a predictable way. Experimental results also indicate that the association behavior of Fv fragments from the monoclonal antibody D1.3 with the lysozyme is extremely similar to that of the entire Fab portion (Poljak, pers. comm.). The electrostatic potential is generated by assigning appropriate point charges to the N-termini and each of the charged residues. The fragment thus has a total of 38 charge sites and is electrically neutral. In a similar study on the diffusion of oxygen ions toward superoxide dismutase (Sines et al., 1990), it has been shown that this prescription of charge assignment gave similar results as more sophisticated models in which each atom was assigned a fractional charge. The time required to calculate the electrostatic field increases by a factor of about three to five depending on the ionic strength if an all-atom model is used for the charge distribution, with most of the extra time spent in generating the boundary conditions, as described below.

From an examination of the crystal structure of the complex (Sheriff et al., 1987), it is seen that the contact surface of the lysozyme with the Fv fragment is relatively flat with the exception of the two side chains from Arg-45 and Arg-68, which fit in the binding groove of the antibody (Kinemage 2). The lysozyme itself is represented as a spherical positive charge that simulates the effect of these residues as they form salt bridges with the antibody. This simple picture of the antigen makes it feasible to test a large number of antibody mutants, providing a more complete global picture of electrostatic steering. The lysozyme, which acts a test charge in the external field of the antibody, is assigned an exclusion radius of 4 Å. For larger values of this parameter, the sphere has difficulty in getting into the binding groove of the antibody, whereas for smaller values, it tends to "stick" near regions of large opposite charge, greatly increasing the time required to run a set of trajectories. This phenomenon has also been observed in diffusional motion simulations by Allison et al. (1988). We have run simulations with the lysozyme charge set at +1e, +3e, and +5e. With the charge set at larger magnitudes, the lysozyme would again stick to portions of the Fv fragment.

The interior of the protein, from which ions are excluded, is assumed to have a dielectric constant of 2. The electrolyte is taken to have a dielectric constant of 78 and an ionic concentration varying from 5 to 350 mM. All calculations are performed for a temperature of 300 K. The relative diffusion constant is determined within hydrodynamic theory (slip boundary conditions) by assigning hydrodynamic radii of 30 Å to the antibody and 4 Å to the sphere and is found to be 0.0695 $Å^2$/ps. The reaction condition is defined in terms of the salt links that are formed in the complex (Kinemages 1, 2), and we will assume that a reaction occurs when the center of the lysozyme is within 8.5 Å of the center of the CD atom in Glu-H50. At this distance, the model lysozyme is in van der Waals' contact with the OE atom of the Glu-H50. The other residue involved in forming salt links with the lysozyme, Glu-H35, is not included in the reaction condition because it lies deeper within the binding groove, and hence the sphere will always encounter Glu-H50 first. This criterion is accurate to the extent that it mimics the contact occurring at the residue level and is representative of the electrostatic steering of the full lysozyme. The Glu-H50 residue is also conserved in a large number of Fv fragments (Kabat et al., 1991), indicating that this study may be relevant for a variety of antibody–antigen systems.

The present system, as already noted, provides a practical means for performing a comprehensive study of the importance of various antibody residues in the efficient electrostatic steering of the antigen. The model parameters involving excluded volumes, diffusion constants, and reaction criteria have been adjusted to yield appreciable reaction probabilities, therefore decreasing the number of trajectories that must be run in order to achieve reliable statistics. Thus, the absolute reaction rates that we obtain are much higher than those expected for diffusion-controlled protein–protein reactions, being on the order of 10^{8-9} M^{-1} s^{-1} for physiological ionic strengths. Although these rates could be lowered by changing the above model parameters, it is our purpose to assess the degree of change in reaction rate induced by a given mutation. For this reason, the emphasis in this study will be on *relative* rates of reaction for mutants in comparison with wild-type diffusion.

Wild-type diffusion

Both aspects of the calculation, the electrostatics portion and the Brownian motion, were performed with the program UHBD, developed by Davis et al. (1990). Shown in Figure 1 is a visual representation of the energy of the ly-

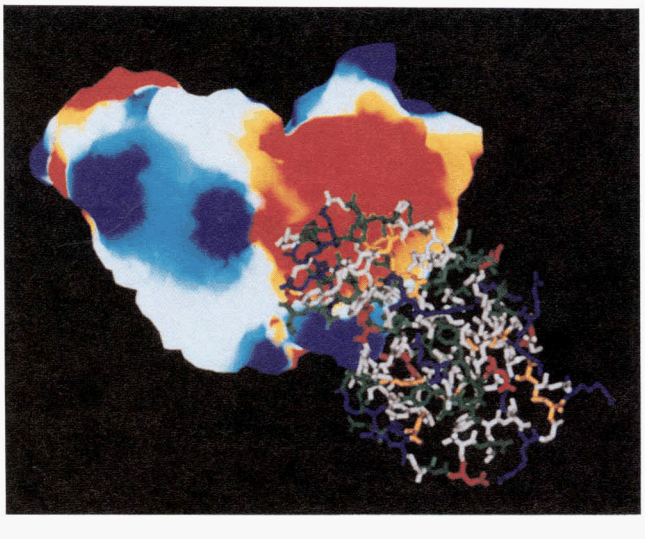

Fig. 1. Binding of the lysozyme within the electrostatic field of the Fv fragment. The red areas indicate attraction of the positively charged lysozyme, and the blue areas show repulsion.

sozyme within the electrostatic field of the wild-type Fv fragment. The reaction site is located within the attractive bulge at the center of the picture, demonstrative of favorable electrostatic steering. This area is flanked by two lobes that indicate repulsive interactions. We have observed that the relative sizes of the bulge and lobes are noticeably affected by point mutations. As an example, Figure 2A gives the electrostatic energy when the negative charge of the Glu-H50 is reversed. For comparison, the wild-type potential for the same molecular orientation is shown in Figure 2B. The field is calculated at an ionic concentration of 150 mM. Drastic changes in the vicinity of the binding site are observed, while the field at more remote points remains largely unaltered. The binding pocket, which is near the bottom of the central red region as seen in Figure 1, is less attractive, indicative of a detrimental effect on electrostatic steering.

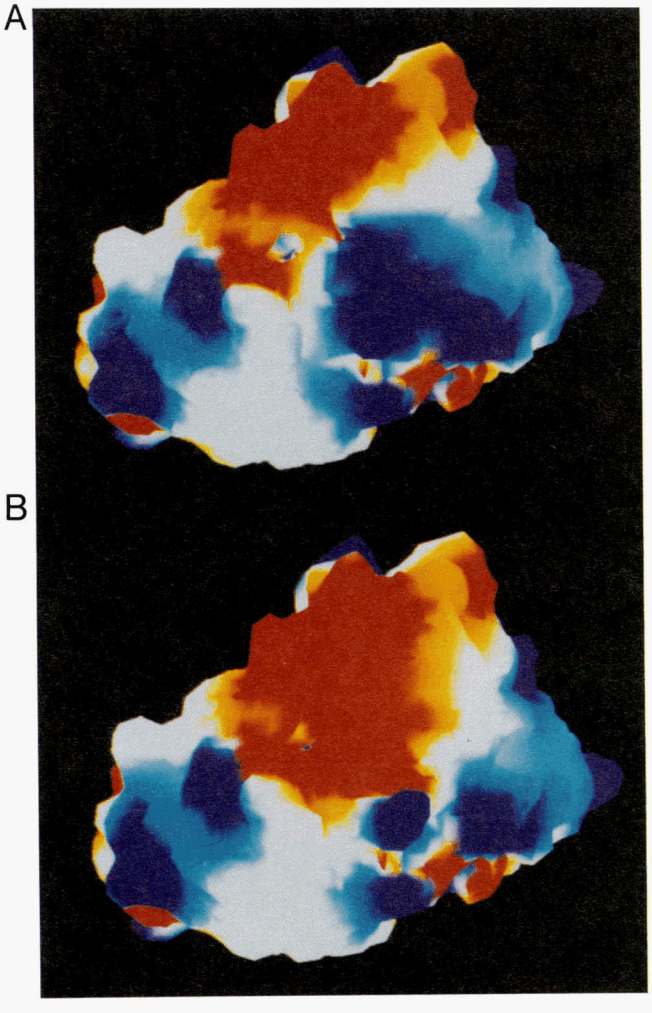

Fig. 2. Visual representation of the electrostatic potential of the Fv fragment when the charge on Glu-H50 is reversed (**A**) and unchanged (**B**). The field is calculated for an ionic strength of 150 mM. The red areas indicate attraction of the lysozyme, and the blue areas show repulsion. The binding region is located at the bottom of the central red area of B, as can be seen by comparing the field map with that of Figure 1.

A histogram of the position of the diffusing sphere can be compiled during the evolution of the trajectories, which represents, in effect, a numerical solution of the Smoluchowski equation (see, for example, the review by Calef & Deutch [1983])

$$kT\nabla^2 C + \nabla C \cdot \nabla U + C\nabla^2 U = 0 \qquad (5)$$

for the steady-state distribution C of a particle undergoing Brownian motion in the presence of an external force-field U. In Figure 3A a slice through three-dimensional space of the logarithm of the distribution for diffusion under the influence of the wild-type potential is displayed. For comparison, a diagram of the negatively charged residues of the antibody fragment in the same orientation as in Figure 3A is shown in Figure 3B. The picture indicates that the diffusing particle tends to random walk until it is "captured" by a region of attractive potential, rather than follow a directed path to the binding site. The concentration clearly shows a maximum within the groove containing the residue Glu-H50. However, also visible is a secondary maximum near the negative-charge cluster defined by the residues L17, L78, L80, L81, and L103 of the antibody (Kinemage 1). This raises the question of whether such areas can act as decoy sites, inhibiting the molecular recognition of an antigen. A weaker hot-spot is also discernible, signaling the presence of local attraction caused by another group of three residues. The noisy character of the plot at larger distances is due to the statistical nature of the simulation.

In order to assess the effect of the total charge of the lysozyme on the molecular recognition between antibody and antigen, we ran simulations for the diffusion of three different charges in the field of the wild-type Fv fragment. The reaction rates relative to that for an uncharged lysozyme are plotted in Figure 4. The enhancement is as much as 65-fold, depending on the values of the charge and ionic strength. The reaction rates give a clear indication of the importance of electrostatic steering in molecular recognition by the antibody, despite the fact that its net charge is zero. As expected, the absolute rates decrease with decreasing charge and increasing ionic strength, although the rate of change with respect to salt concentration is not identical for all values of the charge. As noted by Sines et al. (1990) in a previous study on biomolecular diffusion, this suggests that forces of different length scales contribute to the overall steering effect.

Point mutations of the Fv fragment

As we have adopted a more sophisticated model of the antibody than for the lysozyme it is possible to perform a more thorough study of the effects of site-directed mutations in the Fv fragment on the reaction rate. In order

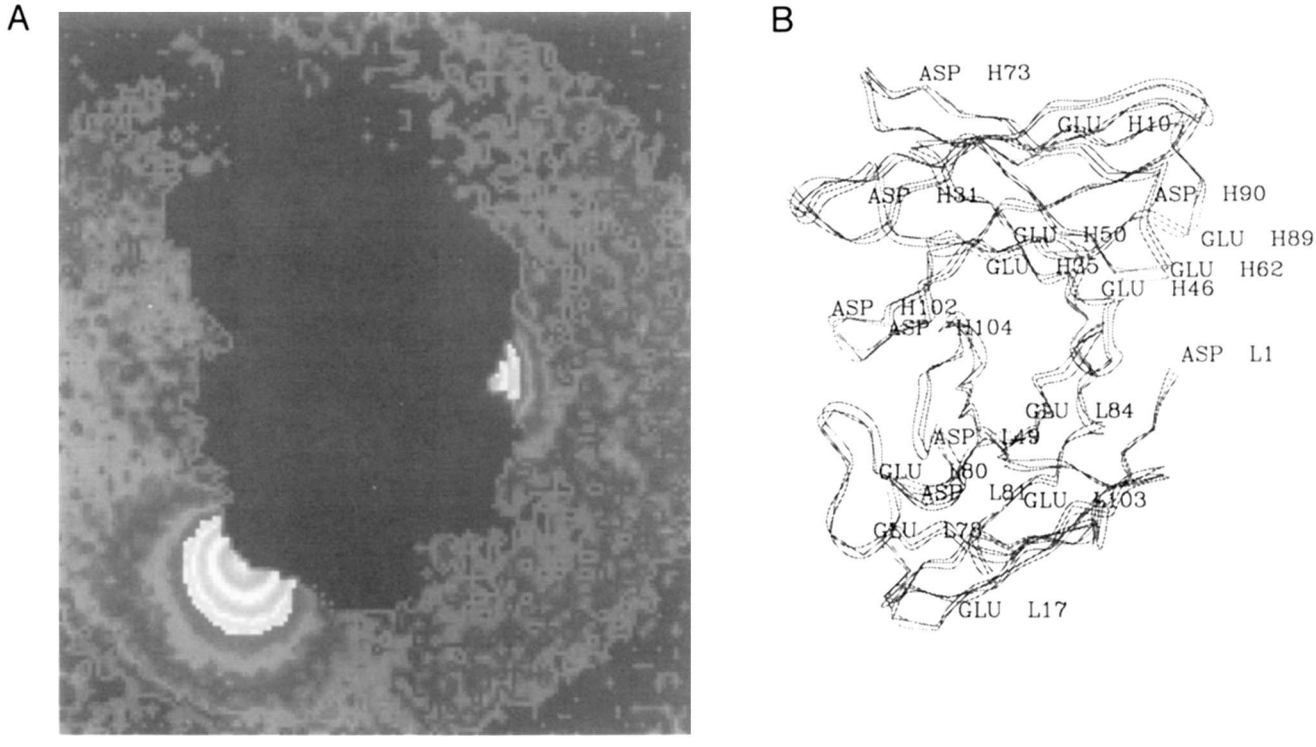

Fig. 3. A: The banded gray-scale representation of the logarithm of the steady-state concentration of the lysozyme around the Fv fragment. The antibody is oriented as in **B**, which also gives the locations of the Glu and Asp residues. The central void is the excluded volume. The white sliver near the center of the picture is the maximum within the binding groove of the antibody. The large white area in the lower left-hand corner is due to local attraction by the charged-residue cluster L17, L78, L80, L81, and L103, a region discernible as a red spot in the electrostatic map of Figure 1.

to obtain a global picture of the fields relevant to molecular recognition, each of the residues Asp, Glu, Asn, and Gln were systematically "mutated" to Asn, Gln, Asp, and Glu, respectively. The location of these residues on an α-carbon trace of the Fv fragment is shown in Figure 5A and B and Kinemage 1. These mutants were constructed by either adding or subtracting a charge from the appropriate site. From the figures, one can see that the above residues are distributed roughly uniformly over the protein, and proceeding in this manner allows us to look at mutations that both constructively and adversely affect the reaction rate. More importantly, our results can be used to predict the particular mutations from the above class that should have the greatest impact on the reaction rate in laboratory experiments. In the results to be displayed below, the lysozyme charge is fixed at +5e, although we have also done simulations with the charge set at +3e and +1e. In each case, the mutants that exert the largest effect during the diffusional motion are the same, and the reason why the +5e results are discussed is that the reaction probability is greater, hence leading to superior statistics.

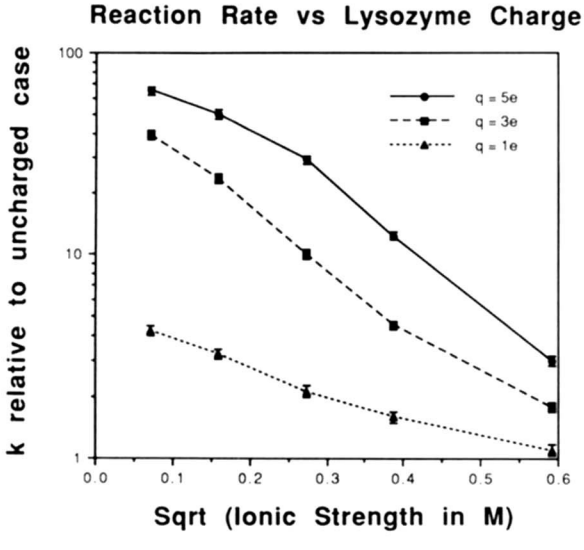

Fig. 4. Reaction rate for the lysozyme with the wild-type antibody as a function of enzyme charge. Rates are given relative to the case where the lysozyme charge is equal to zero.

The primary factor that determines the effect of a given mutation is its distance from the reaction site, with those within about 20 Å having the greatest effect. (This relationship between distance and effect on molecular recognition [Sines et al., 1990; Getzoff et al., 1992] was also found in superoxide dismutase.) Outside of this radius, the reaction rates relative to the wild type are qualitatively similar to those predicted by the Smoluchowski model

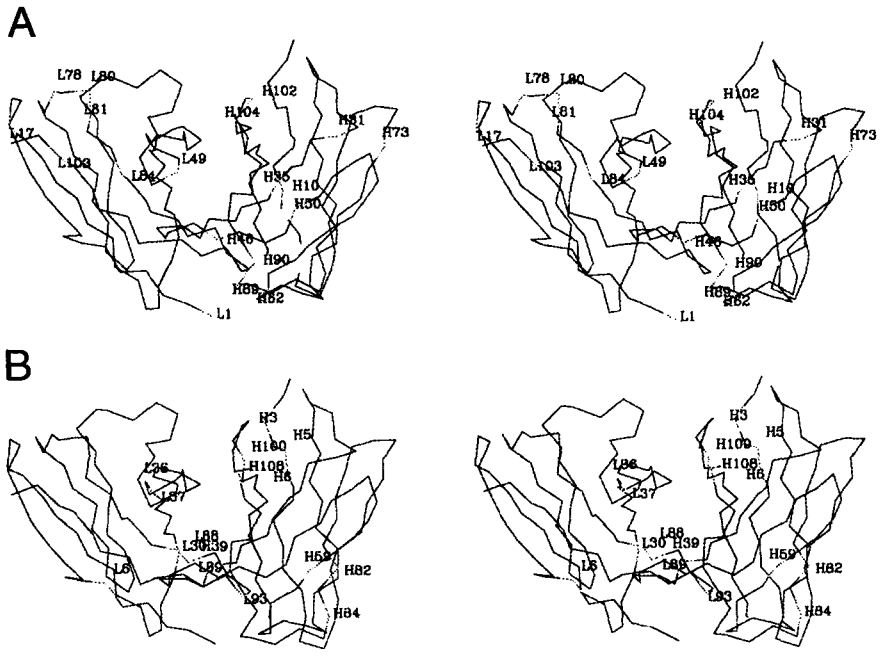

Fig. 5. Stereographic views depicting locations of all of the residues at which point mutations were made. **A:** The Glu and Asp residues, from which a negative charge was subtracted. **B:** The Gln and Asn residues, to which negative charges were added.

(Northrup & Hynes, 1979) for the mutual diffusion of two uniformly charged spheres similar in size to our proteins. In Tables 1 and 2, the reaction rates relative to the wild-type case at 150 mM ionic strength are listed for all of the point mutants that we have investigated. Table 1 depicts the negatively charged mutants that tend to increase the reaction rate over the wild-type rates while Table 2 gives the positively charged mutants that result in lower reaction rates. The relationship between distance and relative rate can clearly be seen in the tables. However, we note that distance from the binding site does not by itself determine the effectiveness of a given mutation. Evidently, electrostatic screening of charge sites by both the protein and the electrolyte also play a role in the molecular recognition process.

Table 1. *Reaction rates for negatively charged mutants*[a]

Mutant	Distance (Å)	Rate
H59:Asn → Asp	5.12	1.91 ± 0.07
L88:Gln → Glu	10.3	1.51 ± 0.06
H100:Asn → Asp	10.9	1.99 ± 0.07
L93:Asn → Asp	11.1	1.22 ± 0.05
L89:Gln → Glu	12.9	1.37 ± 0.06
L30:Asn → Asp	15.5	1.60 ± 0.06
H3:Gln → Glu	18.4	0.94 ± 0.04
H82:Gln → Glu	18.8	1.01 ± 0.05
H84:Asn → Asp	19.0	1.09 ± 0.05
H39:Gln → Glu	19.2	1.10 ± 0.05
H108:Gln → Glu	20.1	1.01 ± 0.05
L37:Gln → Glu	20.2	1.02 ± 0.05
H6:Gln → Glu	21.3	1.01 ± 0.05
H5:Gln → Glu	22.3	1.02 ± 0.05
L36:Gln → Glu	23.6	0.99 ± 0.05

[a] Effects of mutations in which a negative charge is added to the antibody. Distances are from the charge site to the δ-carbon of the Glu-H50 reaction site. Rates given relative to wild-type rates at 150 mM and the errors are statistical.

Table 2. *Reaction rates for positively charged mutants*[a]

Mutant	Distance (Å)	Rate
H50:Glu → Gln	0.00	0.19 ± 0.02
H35:Glu → Gln	4.66	0.34 ± 0.03
H104:Asp → Asn	14.1	0.80 ± 0.04
H31:Asp → Asn	14.1	0.61 ± 0.04
H62:Glu → Gln	14.6	0.93 ± 0.04
H46:Glu → Gln	14.7	1.01 ± 0.05
L49:Asp → Asn	15.5	0.48 ± 0.03
L1:Asp → Asn	16.2	0.88 ± 0.04
H102:Asp → Asn	16.8	0.60 ± 0.04
H73:Asp → Asn	19.7	0.98 ± 0.05
H90:Asp → Asn	20.3	0.96 ± 0.04
H89:Glu → Gln	22.8	0.94 ± 0.04
L84:Glu → Gln	23.5	1.03 ± 0.05
H10:Glu → Gln	23.6	1.03 ± 0.05
L81:Asp → Asn	29.8	0.99 ± 0.05
L80:Glu → Gln	32.1	0.96 ± 0.04
L103:Glu → Gln	33.1	1.00 ± 0.05
L78:Glu → Gln	33.5	1.04 ± 0.05
L17:Glu → Gln	37.6	1.07 ± 0.05

[a] Effects of mutations in which a negative charge is removed from the antibody. Distances are from the charge site to the δ-carbon of the Glu-H50 reaction site. Rates given relative to wild-type rates at 150 mM and the errors are statistical.

The mutations that give a relative rate close to one at physiological ionic strength in Tables 1 and 2 are those that tend to exhibit Smoluchowski properties. This can best be appreciated by studying the relative rates as a function of salt concentration. Two examples, the mutations of Gln-H6 and Glu-L78, are graphed in Figure 6A and B, respectively. For comparison, the relative rates of the Smoluchowski model in which a neutral sphere is increased or decreased by one charge unit are displayed. For the purposes of the plots, the radii of the two spheres were assumed to be 30 Å and 4 Å. It is clear that a better "fit" could be obtained by adjusting the sphere radii. The purpose of the figures, though, is merely to illustrate the qualitative effects of the mutations; they are small at 5 mM (roughly 20% for a lysozyme charge of +5e) and decrease to virtually zero at physiological concentrations.

Within the group that is not described by Smoluchowski theory, the relative reaction rates tend to be larger and exhibit somewhat "nonintuitive" behavior in that they are often larger for higher ionic strengths and lower charges. An explanation of this phenomenon might be as follows. The total potential of the mutated antibody is given by $\phi + \delta\phi$, where ϕ is the wild-type potential, and $\delta\phi$ is the change due to the mutation. (For a point mutation, $\delta\phi$ is simply a monopole field, modified by screening effects.) If ϕ is already an efficient steering field, then a beneficial mutation as represented by $\delta\phi$ will have a small effect. However, if the steering effects of ϕ are relatively weak, then $\delta\phi$ can act as a "beacon" field, giving a greater enhancement of the rate over the wild type. For detrimental mutations, the same argument can be used, reversing the roles of mutant and wild type.

For negatively charged mutants, the largest effects were found at the Asn residues L30, H100, and H59, whose charge sites were 16.7, 10.9, and 5.1 Å, respectively, from the reaction site (Kinemage 1). In some cases, the rate is increased by about a factor of two over the wild-type simulations. The reaction rates relative to wild type for the above mutants are plotted in Figure 7, and it can be seen that the rates are identical for lower salt concentration, indicative of the dominance of long-range effects, and diverge from each other as the ionic strength increases. Interestingly, the largest effects are observed near physiological conditions. Also notable is the change compared to wild type for the Asn-H59 mutation at the highest ionic strength, 350 mM. This phenomenon persists for a lyso-

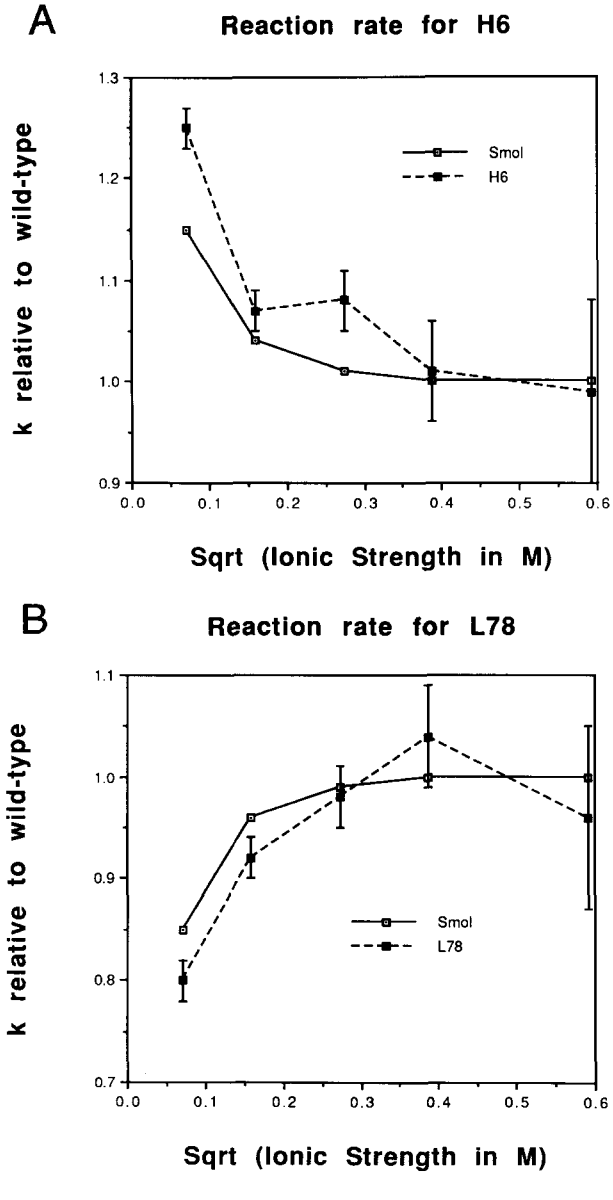

Fig. 6. Reaction rates relative to wild-type for the lysozyme with the Fv mutants Gln-H6 (**A**) and Glu-L78 (**B**). For comparison, the rates as obtained from a Smoluchowski model are also plotted.

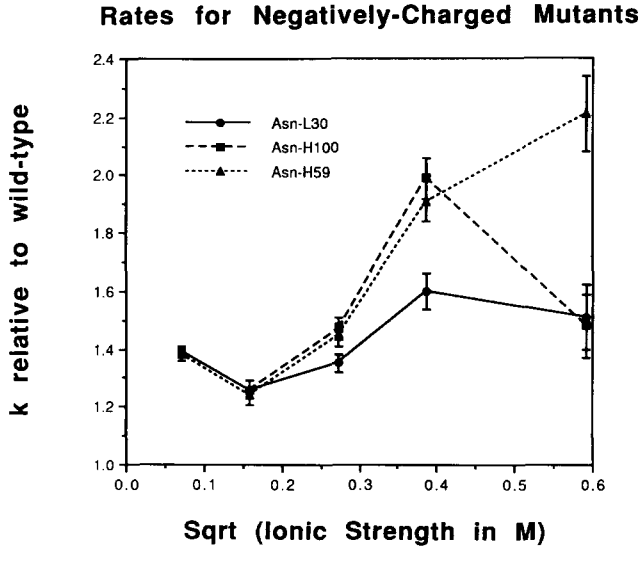

Fig. 7. Reaction rates relative to wild-type for the lysozyme with the Fv mutants obtained by adding a negative charge to Asn-L30, Asn-H59, and Asn-H100.

zyme charge of +3e and is illustrative of the sometimes nonintuitive behavior of the relative rates as discussed above. As stated above, proximity to the reaction site only partly determines the steering effect of a given residue. As an example, addition of a charge at the Asn-L93 residue, which is only 11.1 Å from the Glu-H50 site, yields a smaller relative rate than any of the above changes, although it still exhibits non-Smoluchowskian behavior. The reaction rates for this mutation and that representing the addition of a charge at the Gln-L88 site are shown in Figure 8.

In mutants that carry a net positive charge, the largest effect on reaction rate occurs, as one might expect, when the Glu-H50 residue is neutralized with as much as a 10-fold decrease compared to wild-type rates occurring. Among other mutations, those that give the largest effects are Glu-H35 and Asp-H31 (Kinemage 1). In the full antibody–antigen system, some of the above residues are in contact with the lysozyme, and in such cases the above simulations should be augmented by free-energy calculations in order to calculate the experimental reaction rate. However, this result indicates the importance of steering effects, which should be included in any theoretical prediction of reaction rates. The rates that have been obtained for some of the above mutants are displayed in Figure 9. The ionic strength dependence of the relative rates tends to be smoother than for the negative mutants, except at higher salt concentration where the relative rates are approaching unity. In Figure 10 are plotted relative rates for mutations corresponding to the Asp-L49 and Asp-H104 sites. Again, the relative rates approach one at the highest ionic strengths, although not as quickly as would be expected within the Smoluchowski model.

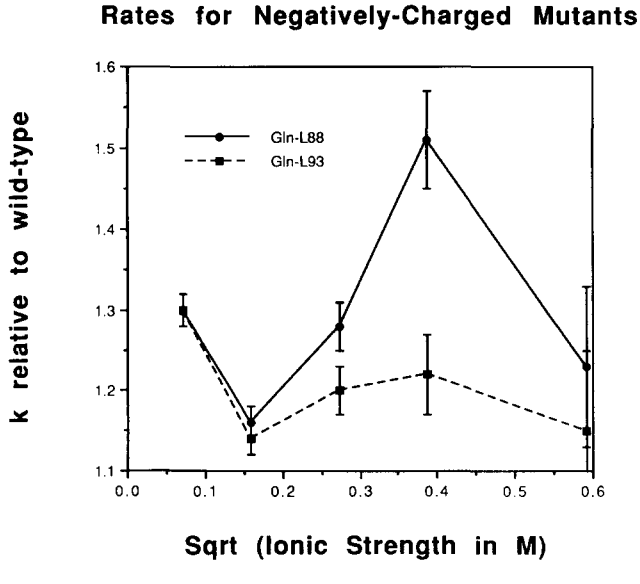

Fig. 8. Reaction rates relative to wild type for the lysozyme with the Fv mutants obtained by adding a negative charge to Gln-L88 and Gln-L93.

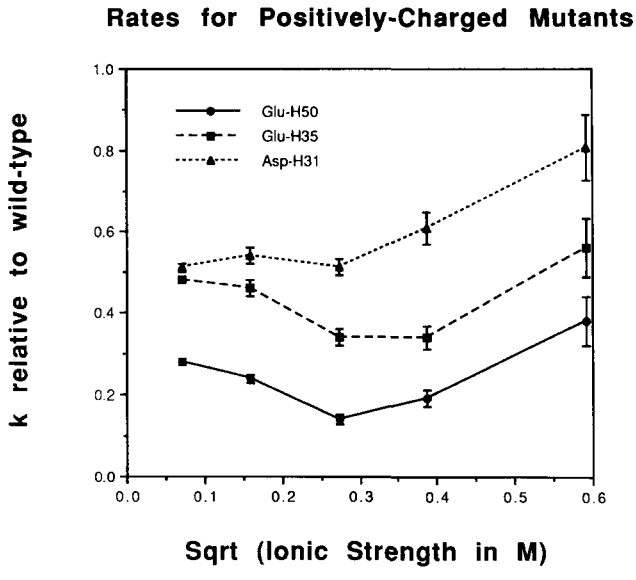

Fig. 9. Reaction rates relative to wild type for the lysozyme with the Fv mutants obtained by removing a negative charge from Asp-H31, Glu-H35, and Glu-H50.

Double mutations

In addition to the more than 30 point mutations discussed in the previous section, we have also considered a limited number of antibody mutants in which two charge sites were altered. In several cases the results of the modifications are well predicted by the multiplicative rule deduced by Sines et al. (1992). In other words, the relative rate for the double mutation is given by the product of the corresponding single-mutation relative rates. In fact, in each instance where at least one of the mutations is of the Smoluchowski-type, the results agree, within statistical error, with the multiplicative model. However, for double mutations that involve two changes of the residues found to be important above in the electrostatic steering, deviations from multiplicative rates are observed. This nonmultiplicative behavior for residues near the active site is also found in the investigation of Sines et al. (1992).

For all of the mutants that we have tested, the one that yields the largest enhancement over the wild-type reaction rate is the double mutation in which charges are placed at the Asn-H59 and Asn-H100 sites. Although the relative rates are not quite as large as those predicted by the multiplicative model, they still represent a nearly threefold increase over the wild-type rates at higher ionic strengths. The results for this mutant are given in Figure 11. For contrast, rates for the double mutant involving the Asn-H100 and Gln-H108 residues are also plotted in the figure. The Gln-H108 mutation alone gives Smoluchowski-like results, and it can be noted that there is very little enhancement of the single Asn-H100 rate at the high ionic strengths, as predicted by the multiplicative model.

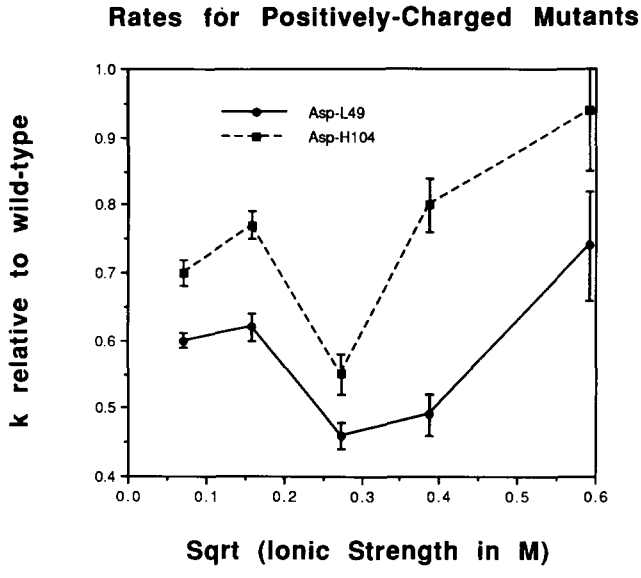

Fig. 10. Reaction rates relative to wild type for the lysozyme with the Fv mutants obtained by removing a negative charge from Asp-L49 and Asp-H104.

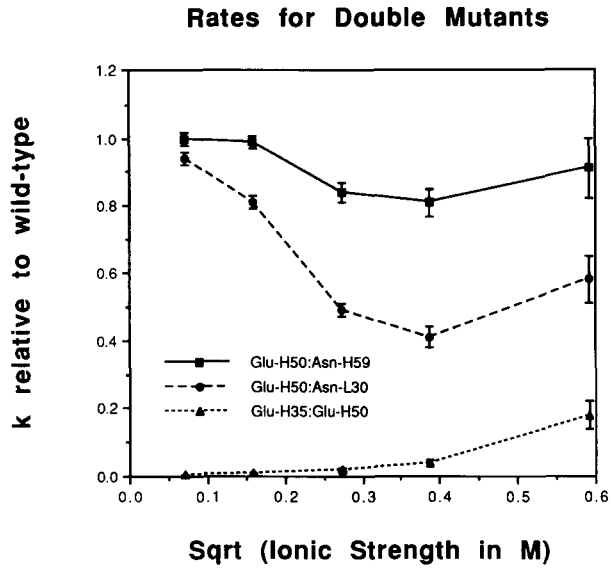

Fig. 12. Reaction rates relative to wild type for the lysozyme with the Fv mutants obtained by modifying the residue pairs Asn-H59:Glu-H50 and Asn-L30:Glu-H5.

We have also run simulations for several double mutations, displayed in Figure 12, involving the neutralization of the crucial Glu-H50 residue. When this is done in conjunction with the addition of a negative charge at the Asn-H59 site, it is seen that the extra charge acts almost as a "surrogate" for recognition of the lysozyme, since the reaction rate is never less than 80% of the wild-type value. A similar kind of mutant, with the Asn-L30 residue replacing the Asn-H59 residue, is less efficient at electrostatic steering, although it still produces increased reaction rates over the single Glu-H50 mutant. Most interesting of the double mutants that we have observed is the one created by removing the charges from both Glu-H35 and Glu-H50, which for all ionic strengths yields reaction rates that are lower than in the uncharged lysozyme case. Therefore, this mutant actively directs the antigen *away* from the binding site. This is also the only case where the absolute rates do not decrease monotonically with decreasing charge and increasing ionic concentration. For the lower ionic strengths, the reaction rate is reduced by two to three orders of magnitude. It is well known, of course, that these residues are important in the binding of the lysozyme because they form part of the salt bridges associated with the complex; however, these simulations suggest that these residues are also very important in the diffusion-controlled step of the reaction.

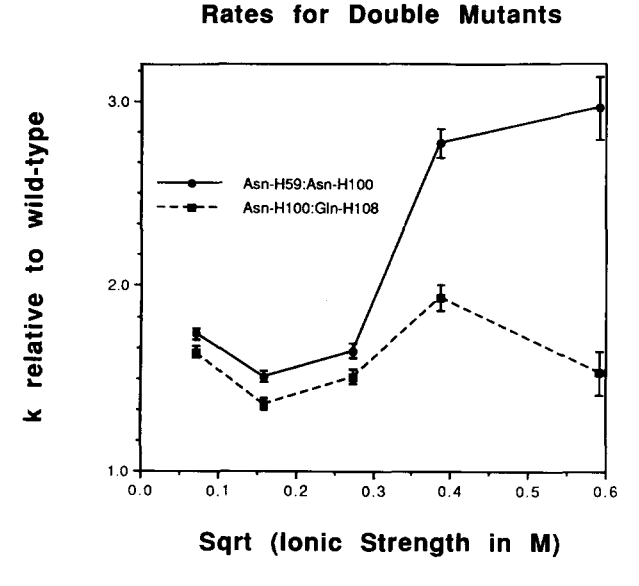

Fig. 11. Reaction rates relative to wild type for the lysozyme with the Fv mutants obtained by modifying the residue pairs Asn-H59:Asn-H100 and Asn-H100:Gln-H108.

We have also employed double mutations to more closely examine the large "hot-spot" in the lysozyme concentration, visible in Figure 3. It is apparent there that the diffusing sphere tends to spend a comparatively large time near a cluster a five negatively charged residues on the antibody, and it was speculated that this might act as a decoy site. However, single point mutations of these residues gave results that were quite consistent with Smoluchowski-like behavior. We also attempted two double mutations in which one of these residues was neutralized in concert with the addition of a charge to a distant neutral residue. One of these two mutants yielded mildly enhanced reaction rates at low ionic strengths with the effect disappearing at physiological strength. This slight change

is most likely due to the subtraction of a dipole field that points away from the reaction site, as it has been shown in a model system that such an arrangement leads to unfavorable electrostatic steering (Northrup et al., 1986). Nevertheless, it is still possible that decoy sites might be important in other antibodies or receptor molecules.

Other mutants

The fact that only mutations within a certain radius of the binding site have a drastic effect on the reaction rate suggests that there exists a "minimal set" of charges that reproduces the electrostatic steering present in the system. In fact, if all charges, positive and negative, more than 20.3 Å distant from the Glu-H50 site are turned off, the result is a slight (from 0 to 20%) enhancement of the native reaction rate at most ionic strengths and lysozyme charges. This reduced set consists of only 20 of the 38 charges on the full Fv fragment. As the radius of the exclusion sphere is increased to 28 Å, encompassing 28 charges of the protein, the reaction rates become very close to the full-protein values. We have computed multipole moments for the two sets of charges described above and compared them with those of the full set, but no similarities were found. This suggests that the key component in molecular recognition is the local character of the field around the reaction site, rather than any global properties of the charge distribution. (We note, however, that the total charge on the antibody still exerts a long-range influence as evidenced by the Smoluchowski-like behavior of distant mutations.) We also note that exclusion spheres with radii less than 20 Å tended to give reduced reaction rates. For example, just including the four closest charges to the binding site (Glu-H35, Glu-H50, Arg-L45, and Arg-L92) yielded reaction rates that were lower by an order of magnitude from those for the wild-type Fv fragment.

As a final simulation, we consider the above-mentioned mutation found in the quail lysozyme in which Arg-68 is replaced by a Lys residue (Smith-Gill et al., 1982). As noted earlier, this change, which shortens the side chain, increases the distance of the positive charge from the negatively charged glutamate residues with which it forms salt links. Because of our simplified scheme for the lysozyme, we have instead performed a similar alteration by moving the negative charge on Glu-H50 from the δ-carbon to the γ-carbon. This decreases the length of the negatively charged side chain from the antibody and mimics a Glu to Asp mutation. For a lysozyme of charge +5e, this gave identical rates to the wild type at 5 mM, but at higher strengths the relative rates decreased monotonically to a value of 0.75 at physiological salt concentration. This behavior is qualitatively similar to that found in the double mutation involving Glu-H50 and Asn-H59, although in the present instance there is a larger adverse effect on the rate. A similar mutation, in which the charge on the Glu-H35 residue is moved, produced a much smaller effect. The relative rates for both of these cases are displayed in Figure 13. Although the results indicate that these mutations can have some effect on electrostatic steering, they also point to the need for free-energy simulations in order to fully understand the large effects associated with them.

Discussion

In this study, we have demonstrated the viability of applying currently available computational methods to the problem of immune recognition. By employing a simplified model for a well-characterized antibody–lysozyme complex, we have been able to calculate relative reaction rates for a wide variety of antibody mutants. This approach has allowed us to map the effect of a given mutation based on its location on the antibody. The charges that are most important in the molecular recognition of lysozyme by HyHEL-5 are in general those closest to the binding site, which has been defined in terms of a residue that is conserved in other antibodies. Effects arising from the mutation of more distant residues are qualitatively described by the Smoluchowski model. As noted above, these studies should be supplemented with calculations such as free-energy simulations in order to fully account for short-range forces and structural effects. In turn though, because the residues most significant in binding interactions between two proteins are also often likely to be important in electrostatic steering, such considerations should be included in any molecular dynamics study.

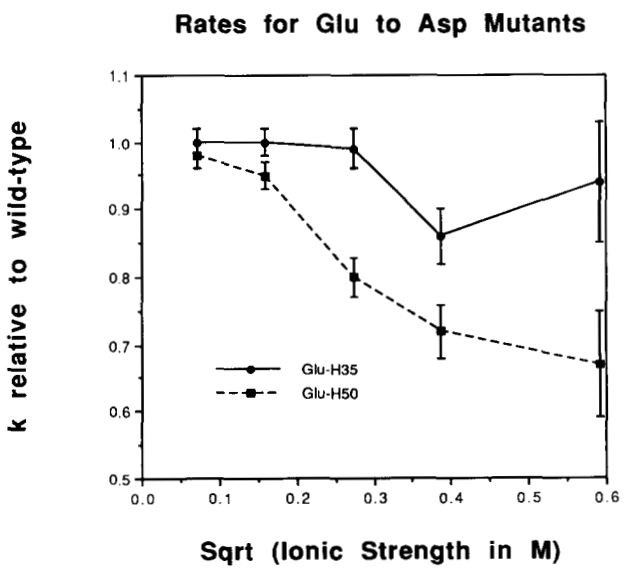

Fig. 13. Reaction rates relative to wild type for the lysozyme with the Fv mutants obtained by moving the charges on the Glu-H35 and Glu-H50, representing Glu to Asp mutations.

We are currently planning, with the help of parallel computers, to implement a more detailed representation of the antigen–antibody system, including a model for the lysozyme that would include orientational effects. In this way, the absolute rate constants that would be obtained from the simulations could be directly compared with laboratory results. Once this has been achieved it should be feasible to utilize the X-ray crystal structures of the other two monoclonal antibodies that have been complexed with lysozyme in order to make comparative investigations. We are also investigating multilevel methods (Holst & Saied, 1993) as a means of solving the full nonlinear Poisson–Boltzmann equation (Holst et al., in prep.). Work is additionally under way to perform both molecular dynamics studies and electrostatic binding calculations of the wild-type HyHEL-5–lysozyme system and various mutants. It appears that Brownian dynamics studies of molecular recognition, in concert with free-energy simulations, and along with information obtained from crystallographic and site-directed mutagenesis experiments can be a powerful tool for providing insight into the rich variety of immune response.

Materials and methods

Electrostatic calculations

The linearized Poisson-Boltzmann equation was solved by discretizing it on a 120^3 grid with 1 Å spacing. For the wild-type case and several mutants, trajectories were run with various grid volumes and spacings to ensure that the above choices yield accurate results. For all mutants, the center of the mesh was placed at the point where the diagonal moments of the quadrupole tensor (Buckingham's definition) vanish for the wild-type case. The atomic radii are taken from the OPLS values (Jorgensen & Tirado-Rives, 1988). In the residue-based charge model, the atomic charge sites are Asp-CG, Glu-CD, Lys-NZ, and Arg-CZ. All histidine residues are assumed to be neutral. The Fv fragment contains two N-termini that are assigned positive charges. At the outer edges of the grid, the boundary conditions were determined by assuming that each charge contributes to the potential as if it were an independent Debye–Hückel sphere of radius 2 Å. It was found that this prescription yielded better convergence for the potential as a function of grid volume than one in which the entire protein was assumed to be a Debye–Hückel sphere. These computations were run on a Cray Y-MP. The UHBD program proved to be highly vectorizable for this task and less than 5 CPU min were required to generate each solution grid.

Diffusional motion

Each trajectory is initiated by placing the lysozyme on a random point of an inner sphere centered on the antibody and is continued until either the reaction condition is satisfied or the diffusing particle crosses the surface of an outer sphere. Throughout the trajectory, the antibody is held rigid and fixed in space. When the lysozyme was sufficiently distant from the Fv fragment that it was beyond the electrostatic grid, an extrapolation of the boundary conditions described above was used to determine the force. As described in the text, the experimentally measurable reaction rate is obtained using the reaction probability and the analytically calculated rates for diffusion to the inner and outer sphere. The radius of the inner sphere is set at 65 Å, and the radius of the outer sphere is taken to be 500 Å. These parameters are determined by gradually increasing each of them until a stable result for the reaction rate is obtained. A variable time step is used depending on the distance of the sphere from the antibody with a minimum value of 10 ps. If a time step results in a collision of the sphere with the protein, it is simply repeated using a new random force. A total of 10,000 trajectories were run for each mutant and at each ionic strength. In order to reduce the statistical error in the relative rates, 100,000 trajectories are used with each charge and ionic strength for wild-type diffusion. The trajectories were run on various SGI workstations, and a set of 10,000 required 2–3 CPU hours.

Acknowledgments

We thank D.R. Davies for providing crystal coordinates for the HyHEL-5–lysozyme complex. We are also grateful to J.A. McCammon for releasing a copy of the program UHBD to us. The figures were generated using the program c3d, written by Chris Culberson of Monsanto Research. This work was supported in part by NIH grant RO1 GM46535 (subcontract from Texas A&M) and by a grant from FMC Corporation. We thank the National Center for Supercomputing Applications for providing computational resources.

References

Allison, S.A., Bacquet, R.J., & McCammon, J.A. (1988). Simulation of the diffusion-controlled reaction between superoxide and superoxide dismutase. II. Detailed models. *Biopolymers 27*, 251–269.

Calef, D.F. & Deutch, J.M. (1983). Diffusion-controlled reactions. *Annu. Rev. Phys. Chem. 34*, 493–523.

Davies, D.R., Padlan, E.A., & Sheriff, S. (1990). Antibody-antigen complexes. *Annu. Rev. Biochem. 59*, 439–473.

Davis, M.E., Madura, J.D., Luty, B.A., & McCammon, J.A. (1990). Electrostatics and diffusion of molecules in solution—Simulations with the University of Houston Brownian dynamics program. *Comp. Phys. Commun. 62*, 187–197.

Davis, M.E. & McCammon, J.A. (1989). Solving the finite difference linearized Poisson-Boltzmann equation: A comparison of relaxation and conjugate gradient methods. *J. Comp. Chem. 10*, 386–391.

Ermak, D.L. & McCammon, J.A. (1978). Brownian dynamics with hydrodynamic interactions. *J. Chem. Phys. 69*, 1352–1360.

Getzoff, E.D., Fisher, C.L., Parge, H.E., Viezzoli, M.S., Banci, L., & Hallewell, R.A. (1992). Faster superoxide dismutase mutants designed by enhancing electrostatic steering. *Nature 358*, 347–351.

Gilson, M. & Honig, B. (1987). Calculation of electrostatic potentials in an enzyme active site. *Nature 330*, 84–86.

Holst, M., Kozack, R.E., Saied, F., & Subramaniam, S. (In prep.). Protein electrostatics: Rapid multilevel solution of the full non-linear Poisson-Boltzmann equation.

Holst, M. & Saied, F. (1993). Multigrid solution of the Poisson-Boltzmann equation. *J. Comp. Chem. 14*, 105-113.

Jorgensen, W.L. & Tirado-Rives, J. (1988). The OPLS [optimized potentials for liquid simulations] potential functions for crystals of cyclic peptides and crambin. *J. Am. Chem. Soc. 110*, 1657-1669.

Kabat, E.A., Wu, T.T., Perry, H.M., Gottesman, K.S., & Foeller, C. (1991). *Sequences of Proteins of Immunological Interest*, 5th Ed. National Institutes of Health, U.S. Department of Health and Human Services, U.S. Government Printing Office, Washington, D.C.

Lavoie, T.B., Kam-Morgan, L.N.W., Hartman, A.B., Mallett, C.P., Sheriff, S., Saroff, D.G., Mainhart, C.R., Hamel, P.A., Kirsch, J.F., Wilson, A.C., & Smith-Gill, S.J. (1989). Structure-function relationships in high-affinity antibodies to lysozyme. In *The Immune Response to Structurally Defined Proteins: The Lysozyme Model* (Smith-Gill, S.J. & Sercarz, E.E., Eds.). Adenine Press, New York.

Nambi, P., Wierzbicki, A., & Allison, S.A. (1991). Molecular interaction between bovine pancreatic trypsin inhibitor molecules probed by Brownian dynamics simulation. *J. Phys. Chem. 95*, 9595-9600.

Northrup, S.H., Allison, S.A., & McCammon, J.A. (1984). Brownian dynamics simulation of diffusion-influenced biomolecular reactions. *J. Chem. Phys. 80*, 1517-1524.

Northrup, S.H., Boles, J.O., & Reynolds, J.C.L. (1988). Brownian dynamics of cytochrome *c* and cytochrome *c* peroxidase association. *Science 241*, 67-70.

Northrup, S.H. & Erickson, H.P. (1992). Kinetics of protein-protein association explained by Brownian dynamics computer simulation. *Proc. Natl. Acad. Sci. USA 89*, 3338-3342.

Northrup, S.H. & Hynes, J.T. (1979). Short range caging effects for reactions in solution. I. Reaction rate constants and short range caging picture. *J. Chem. Phys. 71*, 871-883.

Northrup, S.H., Smith, J.D., Boles, J.O., & Reynolds, J.C.L. (1986). The effect of dipole moment on diffusion controlled biomolecular reaction rates. *J. Chem. Phys. 84*, 5536-5544.

Raman, C.S., Jemmerson, R., Nall, B.T., & Allen, M.J. (1992). Diffusion-limited rates for monoclonal antibody binding to cytochrome *c*. *Biochemistry 31*, 10370-10379.

Sheriff, S., Silverton, E.W., Padlan, E.A., Cohen, G.H., Smith-Gill, S.J., Finzel, B.C., & Davies, D.R. (1987). Three-dimensional structure of antibody-antigen complex. *Proc. Natl. Acad. Sci. USA 84*, 8075-8079.

Sines, J.J., Allison, S.A., & McCammon, J.A. (1990). Point-charge distributions and electrostatic steering in enzyme-substrate encounter: Brownian dynamics of modified copper-zinc superoxide dismutases. *Biochemistry 29*, 9403-9412.

Sines, J.J., McCammon, J.A., & Allison, S.A. (1992). Kinetic effects of multiple charge modifications in enzyme-substrate reactions: Brownian dynamics simulations of Cu,Zn superoxide dismutase. *J. Comp. Chem. 13*, 66-69.

Smith-Gill, S.J., Wilson, A.C., Potter, M., Prager, E.M., Feldmann, R.J., & Mainhart, C.R. (1982). Mapping the antigenic epitope for a monoclonal antibody against lysozyme. *J. Immunol. 128*, 314-322.